Novel edible films of pectins extracted from low-grade fruits and stalk wastes of sun-dried figs: effects of pectin composition and molecular properties on film characteristics

Elif Çavdaroğlu[1] Duygu Büyüktaş[1,2] Stefano Farris[2] Ahmet Yemenicioğlu[1]*

[1]Department of Food Engineering, Faculty of Engineering, Izmir Institute of Technology

35430, Gülbahçe Köyü, Urla, Izmir, Turkey

*Corresponding author: Tel: +90 (232) 7506902, Fax: +90 (232) 7506196,

e-mail: ahmetyemenicioglu@iyte.edu.tr

[2] DeFENS, Department of Food, Environmental and Nutritional Sciences, Packaging Division – University of Milan, Via Celoria 2, 20133 Milan, Italy

Abstract

This study aimed to explore the characteristics of novel fig pectin edible films. For this purpose, films of crude pectin from low-grade sun-dried figs (FP) and crude (SP) and purified pectins (PSP) from stalk waste separated during the processing of high-quality sun-dried figs were evaluated for their physicochemical properties. The properties of pristine (FP, SP, and PSP films) and $CaCl_2$ crosslinked films (FP-Ca^{++}, SP-$Ca^{++}$and PSP-Ca^{++} films) of fig pectins were also compared with films of commercial citrus (CP and CP-Ca^{++}) and apple (AP, AP-Ca^{++}) pectins. The crosslinking improved the mechanical strength and barrier properties of most films. CP, CP-Ca^{++}, PSP, and PSP-Ca^{++} films showed greater mechanical strength and stiffness than other films. PSP-Ca^{++}, PSP and CP-Ca^{++} films showed the lowest water vapor permeability (6.28, 12.85, 14.96 $g.mm.m^{-2}.day^{-1}.kPa^{-1}$, respectively) while SP-Ca^{++}, CP-Ca^{++}, CP, PSP-Ca^{++} films showed the lowest oxygen permeability coefficients (5403, 8265, 10776, 11124 $ml.\mu m.m^{-2}.24h^{-1}.atm^{-1}$, respectively). All crosslinked fig pectin films showed a 2-3-fold lower degree of swelling than CP-Ca^{++} film. The FP-Ca^{++} film showed the highest surface hydrophobicity (contact angle=101.8°), but the lowest water solubility (32.8%) and degree of swelling. Analysis of Pearson's correlations between properties of all pectins and the characteristics of films thereof revealed that galacturonic acid (GA) and RG-I contents affect the mechanical properties, while GA content, degree of esterification (DE), and acetylation affect the moisture barrier performance; finally GA content, linearity of the pectin backbone, and DE affect the oxygen barrier performance of pectin films. Films of stalk waste pectins showed some properties beyond the limits of those obtained from commercial pectins.

Keywords: fig pectin, citrus pectin, edible film, crosslinking, barrier properties, mechanical properties

1. Introduction

Sun-drying is an ancient process that has been used extensively in the Mediterranean region to obtain dried fruits. However, the quality of the final product in this process is highly variable since it is highly affected by climate and field practices. Turkey, with its 85,500 metric tons of production in the 2020/21 season, is the largest producer and exporter of sun-dried figs in the world (Anonymous, 2021). Due to the great variation in their quality, sun-dried figs are classified as extra quality, class I and class II (UNECE, 2016). A considerable part of the fruits is also substandard since they suffer from severe damage caused by insects, rotting, sun-scalding, split and torn, or excessive drying. Recently, a new and rapidly developing trend in processing high-quality sun-dried figs is that the extra quality sun-dried fruits rehydrated to intermediate moisture levels (~35%) are portion packed. Then, they are pasteurized to obtain ready-to-eat, soft, and juicy shelf-stable fruits. The stalks of these premium fruits processed by this emerging method are cut and removed manually before processing. These fig stalks contain part of the flesh tissue that changes between 1 and 1.5% of total fruit weight depending on the experience of workers employed in stalk cutting. Thus, there is an increased industrial interest in the valorization of stalk wastes in the production of value-added products.

Due to their rich soluble dietary fiber content formed mainly by pectin, fig fruits are historically used as a natural laxative and have been considered as a functional food having positive health benefits on gastrointestinal disorders (Trad et al., 2014, Simmons & Preedy, 2016, Rtibi et al., 2018). Therefore, extraction and characterization of pectin from processing wastes of fresh or sun-dried figs have recently attracted considerable interest from different researchers. For example, Gharibzahedi, Smith & Guo (2019a, 2019b) extracted and characterized the molecular and functional properties of pectin from peels of fresh figs. Çavdaroğlu et al. (2020) extracted pectin from whole sun-dried figs and characterized the antimicrobial properties of its emulsion-based edible films with essential oil component

eugenol. Moreover, Çavdaroğlu and Yemenicioğlu (2022) also characterized the molecular and functional properties of fig pectins extracted from whole substandard fruits and stalk wastes of sun-dried figs. Pectin extracted primarily from citrus peels and apple pomace is an indispensable ingredient for the food, biomedical, drug, cosmetics, and nutraceuticals industries, not only due to its techno-functional properties, but also owing to health-promoting effects as soluble fiber (Gilani et al., 2008; Muñoz-Almagro et al., 2020; Noreen et al., 2017; Rezvanain et al., 2017; X. Yang et al., 2015). The molecular architecture and functional properties of pectin from different sources are unique. Thus, studies for extraction of alternative pectins from different fruits and their agro-industrial wastes (e.g., from pomelo, berries, hawthorn, sunflower heads, pomegranate peel, cocoa husk, sugar beet pulp, tomato, carrot pomace, pumpkin waste, passion and banana fruit peels, and watermelon rind, etc.) and characterization of their functional properties have become a popular research topic (Henao-Díaz et al., 2021; Marić et al., 2018; Dranca & Oroian, 2018; Gamonpilas et al., 2021; Li et al., 2021; Muñoz-Almagro et al., 2021; Reichembach & Lúcia de Oliveira Petkowicz, 2021).

This study aimed to explore the characteristics of novel fig pectin edible films. For this purpose, pristine and $CaCl_2$ crosslinked films of crude pectin from whole low-grade sun-dried figs and crude and purified pectin from stalk wastes separated during sun-dried fig processing were evaluated for their detailed physicochemical properties such as solubility, swelling, hydrophobicity, mechanical and barrier properties, color and transparency, and morphological features. The properties of fig pectin films were also compared with those of commercial citrus and apple pectin films. The relevance of this work lies in the fact that it is the first study showing the advantages of fig pectin edible films over currently used commercial pectin films. Moreover, this is the first report that investigates the effect of pectin composition and molecular properties on the physicochemical characteristics of obtained edible films by analyzing Pearson's correlation coefficients.

2. Materials and methods

2.1. Materials

Citrus pectin (CP, P9135, galacturonic acid ≥ 79%, methoxy content ≥ 8%) was obtained from Sigma-Aldrich (St. Louis, MO, USA). Apple pectin (AP) was obtained from Tito (Turkey). All other chemicals were reagent grade. The cut stalk waste (contains stalk and a piece of fruit flesh that accounts for 1 to 1.5% of total fruit flesh weight) of high-quality sun-dried figs (Cultivar Sarılop) separated during processing (fig stalk), and the lowest quality substandard sun-dried figs (Cultivar Sarılop) which are mainly processed into the paste (low-grade sun-dried figs) were kindly supplied by KFC Gıda Tekstil Sanayi İthalat İhracat Yatırım A.Ş (Menemen, Turkey). All samples used were fluorescence tested in the factory to ensure that they were free from mycotoxins. The samples were kept at -20ºC until they were used for pectin extraction.

2.2. Methods

2.2.1. Pectin extraction

Crude pectin was extracted from low-grade substandard fruits or stalk waste at the optimal conditions reported by Çavdaroğlu et al. (2020) using a 6.0% (w/v) citric acid (CA) water solution at 95ºC for 1 hour. The pectin in the extract was precipitated with pure ethanol (pectin extract:ethanol ratio= 1:2, v/v) and collected by centrifugation (22,668 xg for 10 min). The crude pectins (FP and SP) were obtained by drying the collected precipitates for 24 h at 40 °C. The pure pectin (PSP) was obtained by suspending alcohol precipitated pectin in distilled water and stirring the resulting slurry with a glass rod for 10 min. The pectin was then again precipitated with ethanol (slurry:ethanol ratio=1:1, w/w) and then collected by centrifugation. This procedure (washing with water and alcohol precipitation) was repeated twice. The purified pectin was dried for 24 h at 40 °C.

2.2.2. Molecular properties and composition of pectins

Galacturonic acid content (GA) was determined spectrophotometrically by the classical m-hydroxydiphenyl method using D-galacturonic acid as a standard (Blumenkrantz & Asboe-Hansen, 1973). Sugar composition (glucose, arabinose, galactose, and rhamnose) of pectins was also determined spectrophotometrically using specific enzymatic kits (for glucose: GAGO20 glucose assay kit of Sigma-Aldrich, St. Lous, MO, USA; for arabinose/galactose and rhamnose: K-ARGA and K-RHAMNOSE kits of Megazyme Ltd., Ireland, respectively). Degree of esterification (DE) and degree of acetylation (DA) of pectins were determined by the classical titrimetric and HPLC methods described in our previous work, respectively (Çavdaroğlu & Yemenicioğlu, 2022). Sugar molar ratios [R-1 (mol%, linearity of pectin)= GalA (mol%)/(Rha (mol%) + Ara (mol%) +Gal (mol%), R-2 (mol%, RG-I fraction content of pectin)= Rha (mol%)/GalA (mol%), R-3 (mol%, degree of branching of RG-I) = (Ara (mol%) + Gal (mol%))/Rha (mol%), R-4 (mol%, length of Gal branching in RG- I) = Gal (mol%) /Rha (mol%)] were calculated according to Denman & Morris, (2015). Moisture and ash contents were determined according to AOAC (AOAC, 1990). Soluble protein contents of pectins were determined by the Bradford method (Bradford, 1976). Total carbohydrates were determined spectrophotometrically by the phenol-sulfuric acid method using D-glucose as a standard (Dubois et al., 1956). The phenolic content of extracted pectin was determined spectrophotometrically at 760 nm using the Folin–Ciocalteu's reagent as a reactive compound and gallic acid (GAE) as a standard (Singleton & Rossi, 1965). All analyses were performed in triplicate.

2.2.3. Film preparation

For the preparation of films, solutions of different pectins at 3% (w/v) were heated using a hot plate working under continuous stirring at 60°C for 30 minutes. The solutions were then cooled to room temperature and further treated at 10,000 rpm for 1 minute using a homogenizer-

disperser (Heidolph, Germany, rotor ϕ = 6.6mmTip). Then, 0.9 g glycerol (30% w/w of pectin) was added as a plasticizer, and the mixture was stirred for 15 minutes. The solution was further homogenized at 10,000 rpm for 4 minutes using the homogenizer-disperser. To obtain solution-cast pristine films, 20 g portions of film solutions were poured into glass Petri dishes (inner diameter 10 cm) and the dishes were dried in a controlled test cabinet at 25°C and 50% RH for 24 hours. The crosslinked films were obtained by treating dried films with 3% (w/w) $CaCl_2$ solution and drying films again in the controlled test cabinet at 25°C and 50% RH for 24 hours (Rezvanain et al. 2017). The pristine and crosslinked films of crude pectins from low-grade whole substandard fruits and stalk waste were designated FP and FP-Ca^{++}, and SP and SP-$Ca^{++,}$ while pristine and crosslinked films of purified pectin from stalk waste were designated PSP and PSP-Ca^{++}, respectively. The pristine and crosslinked commercial citrus and apple pectins films were designated CP and CP-Ca^{++}, and AP and AP-Ca^{++}, respectively. All pectin films were prepared in duplicate.

2.2.4. Mechanical properties of films

Tensile strength at break (TS), elongation at break (EAB), and Young's modulus (YM) of films were determined using a Texture Analyzer TA-XT2 (Stable Microsystems, Godalming, UK) according to ASTM Standard Method D 882-02 (ASTM, 2002a). The dried films were conditioned in a controlled test cabinet at 25°C and 50% relative humidity (RH) for 24 hours before testing. Then, the films were cut into 50-mm-long and 8-mm-wide strips. The initial grip distance was 50 mm, and the drawing speed was 50 mm / min. Minimum eight strips of each film were tested. The thickness of films was measured by using a micrometer (Chronos, UK).

2.2.5. Water vapor permeability of films

The WVP of pectin films was measured using Payne permeability cups (Elcometer 5100, England) according to the ASTM Standard Method E96 (ASTM, 2016). Each cup was filled with 3 g of dried silica beads. A film (diameter: 6 cm) and an o-ring were placed on top

of each cup, and cups were sealed with a metal ring with three screw clamps. The cups were weighed and then placed in a controlled test cabinet (TK 120, Nüve, Turkey) working at 25 °C and 60% RH. The cups were weighted periodically for 72 h, and the measured weights were plotted against time. The linear portions ($R^2 \geq 0.99$) of the curves with at least five data points were used for the calculation of WVP according to equation 1.

$$WVP = \frac{G\,L}{A\,t\,S\,(R_1 - R_2)} \qquad \text{(eq.1)}$$

where G is the weight change from the straight line (g), L is the thickness of the film (mm), t is the time (day), A is the test area (m^2), S is the saturation vapor pressure at test temperature (3.169 kPa at 25 °C), R_1 the relative humidity of the test chamber (60%) and R_2 the relative humidity in the dish (0%). Four independent tests per film were performed.

2.2.6. Oxygen barrier properties of films

The oxygen barrier properties of the films were evaluated in terms of the oxygen transmission rate (*OTR*, expressed as mL m^{-2} $24h^{-1}$) using a Totalperm permeability analyzer (ExtraSolution® Srl, Capannori, Italy) equipped with an electrochemical sensor and based on the isostatic method, according to the standard method of ASTM F1927 at 23° C and 75% RH. Specimens were sandwiched between two aluminum-tape masks, allowing a surface of 2.01 cm^2 to be exposed to the permeation of oxygen. All the tests were carried out with a carrier flow (N_2) of 35 mL min^{-1} and at 1 atm oxygen partial pressure difference on the two sides of the specimen. To reset any difference in the *OTR* values possibly arising from different thicknesses of the specimens, *OTR* values were converted to a permeability coefficient ($P'O_2$) according to equation 2 (Uysal Unalan et al., 2015):

$$P'O_2 = PO_2 \times t = \frac{OTR}{\Delta p} \times t \qquad \text{(eq. 2)}$$

where $P'O_2$ is the oxygen permeability coefficient (mL.µm.m^{-2}.24h^{-1}.atm^{-1}), PO_2 is the permeance (defined as the ratio of the *OTR* to the difference between the partial pressure of the vapor on the two sides of the film, Δp), and t is the total thickness of the material. Each *OTR* value was from three replicates.

2.2.7. Film solubility

Before determining their solubilities, the moisture content of the films was determined by the vacuum oven method applied at 70ºC and 16.9 kPa for 24 h. Eight pieces of each film were measured for their moisture contents. The solubility of films was determined according to the method described by Pérez et al. (2016). Briefly, pieces of films (15 × 7.5 mm^2) were placed into a test tube with 10 mL of distilled water. The tubes were then shaken at 240 rpm for 24 h using an orbital shaker (IKA, OS 5 basic, Germany) and placed in an incubatorat 25 ºC and 50% RH. After that, the remaining solids in the tubes were collected by filtration. The insoluble dry matter content was determined by hot air drying at 105 ºC until reaching constant weight. The film solubility (%) was determined from equation 3:

$$\text{Film solubility (\%)} = 100 \times \frac{(\text{Initial dry matter} - \text{Insoluble dry matter})}{\text{Initial dry matter}} \qquad \text{(eq.3)}$$

Eight pieces from each film were tested for their solubility.

2.2.8. Degree of film swelling

The degree of swelling of the films was determined by the gravimetric method. The films (30 × 10 mm^2) held in distilled water at room temperature were drained and weight periodically at 7.5, 15, and 30 min. The degree of swelling (SW) was determined using equation 4:

$$SW = 100 \times \left(\frac{(W_W - W_D)}{W_D}\right) \qquad \text{(eq. 4)}$$

where W_D is the weight of dried film; W_W is the weight of the swelled film. Three pieces from each film were tested for their swelling degree.

2.2.9. Wettability of films

Wettability of pectin films was assessed by water contact angle measurements, which were performed using an optical contact angle apparatus (OCA 15 Plus, Data Physics Instruments GmbH, Filderstadt, Germany) equipped with a high-resolution CCD camera and a high-performance digitizing adapter. SCA20 software (Data Physics Instruments GmbH, Filderstadt, Germany) was used for the image capturing and contact angle determination. Rectangular specimens (3 × 1.5 cm^2) were kept flat throughout the analysis, and the contact angle of water in the air (θ, °) was measured by gently dropping a droplet of 4.0 ± 0.5 mL of Milli-Q water (18.3 MV cm) onto the pectin films surface at 23 ± 1 °C and 50 ± 2% RH. The experiments were done in triplicates.

2.2.10. Morphological properties of films by AFM and SEM

The surface topographical images of films were obtained by atomic force microscopy (AFM, MMSPM Nanoscope 8 from Bruker, USA) in an intermittent-contact mode in the air with silicon tips (resonance frequency ≈340 kHz, spring constant ≈40 N m-1, tip radius 8 nm). The captured images (minimum 4 for each sample) were analyzed by Nanoscope Analysis software v.1.5 (Bruker, USA). The surface roughness (R_{rms}) was calculated from Equation 5 as the root mean square average of height deviations (Z_i) taken from a mean data plane ($\underline{Z}$).

$$R_{rms} = \sqrt{\frac{\sum_{i=1}^{N}\left(Z_i - \underline{Z}\right)^2}{N-1}} \qquad (eq.\,5)$$

The R_{max} parameter indicates the maximum vertical distance between the highest and the lowest points in the image.

The surface and cross-sectional morphologies of pectin films were also examined using a scanning electron microscope (SEM, 250 Quanta FEG, FEI Company, USA). Before the experiment, the films were first freeze-dried and then placed into liquid nitrogen and crashed for the SEM examination. After that, the samples were gold-coated with a sputter coater (Emitech K550X, Quorum Technologies Inc., UK) at 10 mA for 60 s.

2.2.11. Transparency and color of films

Film transparency was determined according to ASTM D-1746 (2002b) with modifications of the method described by Pérez et al. (2016). The transparency of films was measured at 600 nm using a spectrophotometer. Rectangular pieces of films (30 × 10 mm^2) were placed into the spectrophotometer cell, and readings were taken against the empty cell used as a blank. Eight replicates of each film were tested. Transparency was calculated from Equation 6.

$$T_{600} = \frac{(\log \%T)}{b} \qquad (eq.\ 6)$$

where b is the film thickness (mm).

The color of films was determined using a colorimeter (CR-400, Minolta Sensing, Osaka, Japan) and recording the L*, a*, b* values

2.2.12. Statistical analysis

Statistical difference between treatments was determined by using variance analysis (one way-ANOVA) and Fisher post-hoc test ($p \leq 0.05$) using Minitab (ver.18.1, Minitab Inc., United Kingdom). Pearson's correlation tests were carried out to investigate the interrelationships between the pectins' compositional or molecular properties and the film properties.

3. Results and discussions

3.1. Composition of pectins

The composition of pectins obtained from whole low-grade and substandard sun-dried figs (FP) and stalk waste (composed of a stalk and adjacent fruit flesh) separated during the processing of high-quality sun-dried figs (SP) were compared with those of commercial citrus (CP) and apple (AP) pectins (Table 1). The highest total carbohydrate content was determined for CP (89.1%), followed by AP (83.2%) and SP (82.0%). The FP showed the lowest total carbohydrate content (58.9%), but the highest ash (~8.2%) and soluble protein (~11%) contents originated mainly from many tiny seeds (florets) within the fruit flesh (Çavdaroğlu and Yemenicioğlu 2020). The high ash content determined for fig fruit pectin is also compatible with the literature, whereby figs were reported to be a good source of minerals (Trad, Bourvellec, et al., 2014). The SP obtained from stalk waste lacked seeds. Thus, it showed a similar composition to AP and CP. Therefore, the purified pectin (PSP) was obtained using stalk wastes. The SP and its purified form PSP contained similar ash and soluble protein contents ($p>0.05$). The soluble protein contents of SP and PSP are only slightly higher than that of CP, but significantly higher (1.7-2-fold) than that of AP. The sun-dried Sarılop figs used in the current study are also known as a good source of polyphenols (Kelebek et al., 2018). The polyphenols form a complex with polysaccharides like pectin through hydrophobic interactions (Liu et al., 2020; Tang et al., 2003). After that, the complex is stabilized with hydrogen bonds formed mainly between hydroxyl groups of polyphenols and oxygen atoms in different groups/linkages of polysaccharides (e.g., carboxyl/carboxylic acid and hydroxyl groups, the oxygen atom of glycosidic linkages) (Jakobek, 2015; Liu et al., 2020; Wu et al., 2009). In the current study, the highest total phenolic content (TPC) was determined for PSP (1.82 g GAE/ 100g), followed in descending order by FP, SP, CP, and AP. However, it should be noted that

the TPCs of fig pectins in the current work were significantly lower than the TPC of ~3.0 g GAE/ 100 g determined for pectin extracted from peels of fresh figs (Gharibzahedi et al. 2019b).

3.2. Molecular properties of pectins

The GA of pectins varied between 32.4 and 78.8%. The CP showed the highest GA (78.8%) while AP had intermediate GA (50.4%), and crude pectins, SP (34.3%), and FP (32.4%) had the lowest GAs. It is important to note that the GAs determined for crude pectins extracted from sun-dried figs and their stalks were in the range of those (24.5-33.4%) determined by Trad et al. (2014b) for pectic compounds extracted from different fresh Tunisian fig cultivars. In contrast, the purified stalk waste pectin PSP showed a 1.8-fold higher GA content (63%) than its crude form (SP) and ranked second in GA after CP. Considering the DE values, the CP, AP and PSP could be classified as high-methoxyl pectins (HMP, DE>50%), while SP and FP are low-methoxyl pectins (LMP, DE<50%). The increased DE of PSP with purification could be attributed to the increased proportion of high methoxyl GA fractions by insolubilization of LMP fractions during repeated solubilization-alcohol precipitation cycles. It is also noteworthy that the GA and DE of PSP are higher than those of fresh fig peel pectin (GA: 52.5%, DE: 39%) obtained with hot acidic extraction by Gharibzahedi, Smith & Guo (2019a). The DA of pectins used in the current work also showed a great variation between 2.7% and 29.9%. The fig pectins showed significantly higher DA than commercial pectins. The PSP showed the highest DA. Thus, it appears that the purification eliminated not only LMP fractions, but also pectin fractions with low DA. The DE and DA are highly effective in gelation and emulsifying properties of pectins (Broxterman et al., 2017; Schmidt et al., 2015; Vriesmann & Petkowicz, 2013). However, data about the effect of DA on film properties of pectin are scarce. In the literature, the DAs of some pectins were given as follows: 3% for citrus and 14% for pear pectins (Voragen et al., 1986), 18-58% for okra pectins (Sengkhamparn et al., 2009),

17% for cacao pod husk pectin (Vriesmann & Petkowicz, 2013), 20% for carrot pectin (Broxterman et al., 2017), and 16-46.2% for sugar beet pectin (Bindereif et al., 2021).

The sugar molar ratios (R1, R2, R3, and R4) of pectins were also estimated by determining the amount of major sugars in fig pectins, D-glucose (D-Glu), L-rhamnose (L-Rha), D-galactose (D-Gal), and L-arabinose (L-Ara) (Çavdaroğlu et al. 1999). The D-Glu content of SP, FP, and AP did not vary considerably and changed between 6.07 and 6.48%, while CP obtained from citrus peels contained a limited D-Glu content. It is also important to report that the purification caused almost 3.6-fold lower glucose content for PSP than SP, which is the crude form of PSP. The CP and FP showed low levels of L-Rha while AP, SP, and PSP contained significantly higher L-Rha (3 to 7-fold) than these two pectins ($p<0.05$). The highest D-Gal content was found for PSP (6.3%), followed by slightly to moderately lower D-Gal contents of FP, CP, and SP, and considerably lower D-gal content of AP (1.5%). Finally, the CP, FP, SP, and PSP contained similar L-Ara contents ($p<0.05$) changing between 3.78 and 4.92%, while AP contained significantly lower L-Ara content (1.8%) than these pectins.

In majority of the pectins, the main structural fraction is formed by homogalacturonan (HG, ~65%), while rhamnogalacturonan-I (RG-I, ~20-35%) is the second dominant structural form, and rhamnogalacturonan-II (RG-II, ~10%) is the minor fraction (Alba & Kontogiorgos, 2017; Basak & Annapure, 2022; Chandrayan, 2018; Yapo, 2011). Since RG-II is a very complex minor fraction composed of many different sugars, it is not considered in the theoretical calculations (Houben et al., 2011; M'sakni et al., 2006). The R-1 values suggested that the AP and CP showed the highest molecular linearity while PSP had intermediate linearity, and FP and SP had the lowest linearity. According to R-2 values, the SP showed the highest RG-I content, followed by almost 2, 2.3, 3.5, and 18.5-fold lower RG-I contents of AP, PSP, FP, and CP, respectively. The R3 and R4 also suggested that the degree of branching and D-

Gal branch length of RG-I for pectins in descending order were as follows: CP, FP, PSP, SP, and AP.

3.3. Mechanical properties of pectin films

Mechanical properties of pristine and $CaCl_2$ crosslinked films obtained from fig and commercial pectins are shown in Table 2. Although the crosslinking caused a significant reduction in thickness of all film, the average thicknesses of pristine and crosslinked films of citrus and fig pectins changed at a very narrow range between 84.1 and 89.0 µm and 71.2 and 78.4 µm, respectively. In contrast, pristine and crosslinked AP films were significantly thinner than all of the other respective pectin films. The results obtained for pristine films showed that the CP and PSP films had the highest tensile strengths (TSs), while AP and SP films showed 2.4-2.8-fold lower TSs, and FP showed 5-5.7-fold lower TS than those of CP and PSP films. The crosslinking improved the TSs of some films significantly. For example, AP-Ca^{++}, CP-Ca^{++}, and FP-Ca^{++} films showed 1.3-, 1.6- and 1.7-fold higher TSs than their pristine AP, CP, and FP films, respectively. In contrast, no significant differences were determined between TSs of SP and SP-Ca^{++} and PSP and PSP-Ca^{++}. Thus, it seemed that the crude and purified stalk waste pectins lacked a block-wise distribution for deesterified carboxyl groups that was essential for the formation of a stable egg-box model (Fraeye et al., 2009). The CP-Ca^{++} showed the highest TS among crosslinked films followed in descending order by TSs of PSP-Ca^{++}, AP-Ca^{++}, SP-$Ca^{++,}$ and FP-Ca^{++}. The SP, AP, and FP gave the most flexible pristine films with elongation at break (EAB) values of 26.2, 21.9, and 15.2%, respectively. The PSP films showed limited flexibility (EAB: 8.8%), while CP gave almost no flexibility (EAB: 4.2%). The crosslinking caused a significant reduction (1.8 to 3.7-fold) in EAB of most pectin films, except for CP films that gave similar EAB for pristine and crosslinked films. According to Young's modulus (YM) values, the CP-Ca^{++} and PSP-Ca^{++} films were the stiffest films, followed in descending order by CP and PSP films showing intermediate stiffness and by AP-Ca^{++}, SP-

Ca^{++}, CP-Ca^{++}, SP, FP, AP films showing lower-intermediate to low stiffness. The overall results clearly showed that pristine and crosslinked films of PSP and CP showed similar mechanical properties, whereas pristine and crosslinked films of SP and FP showed similar or slightly different mechanical properties with AP. Moreover, it is also evident that the purification of SP and use of obtained PSP in film making caused significant improvements in the mechanical strength of fig stalk waste pectin films.

In the literature, edible films from different pectins have also been characterized for their mechanical properties. For example, pristine films from pomegranate peel (3%, v/w), pineapple peel (3%, v/w), and lime peel (1%, v/w) pectins showed TS values of 2.42, 5.60, and 16.93 MPa, and EAB values of 6.55, 14.84 and 1.77%, respectively (Oliveira et al., 2016; Rodsamran & Sothornvit, 2019a, 2019b). These results suggested that the pristine films of pomegranate peel and pineapple peel pectins had comparable mechanical properties with pristine films of FP and SP pectins, respectively, while films of lime peel pectin showed comparable mechanical properties with films of PSP. Data related to $CaCl_2$ crosslinked pectin films are scarce. However, it was reported that the pectin obtained from mango peel could not form a film in the presence of $CaCl_2$ (Chaiwarit et al., 2020). In contrast, edible films obtained from pumpkin peel pectin (5%, v/w) showed a TS of 5.28 MPa and EAB of 14.37% after $CaCl_2$ crosslinking (Lalnunthari et al., 2020).

The calculated Pearson's coefficient of correlations (r) showed the factors (composition and molecular properties of pectins) affecting the mechanical properties of pristine and crosslink films separately (see supplementary files Table S1 and S2). The most significant positive correlations were determined between GA of pectins and TSs (r= 0.895 and 0.937) and YMs (r= 0.0887 and 0.936) of pristine and crosslinked films, respectively. Moreover, a moderate positive correlation was also determined between the DE of pectins and TS of pristine films (r= 0.723). As expected, significant negative correlations also existed between GA of

pectins and EAB of pristine (r= -0.868) and crosslinked (r= -0.822) films. These results clearly showed that the GA is the primary factor giving the mechanical strength and stiffness of both pristine and crosslinked films. Interestingly, the R-2 (RG-I content) of pectins correlated positively with EAB of pristine and crosslinked films (r=0.805 and 0.779), respectively. Thus, it seemed that the presence of RG-I interfered with the formation of rigid entanglements in film network created by linear homogalacturonan chains, thus, films turned more flexible by increased chain mobility.

3.4. Water vapor barrier properties

Water vapor permeability (WVP) values of different pectin films are given in Table 3. The WVP of films showed a great variation and changed between 6.3 and 31.7 $g.mm.m^{-2}.day^{-1}.kPa^{-1}$. The PSP-$Ca^{++}$ with its 2 to 5-fold lower WVP than those of other films showed the best moisture barrier effect. The PSP, CP-$Ca^{++,}$ and FP-Ca^{++} films showed intermediate moisture barrier effects, while SP-Ca^{++}, CP, and AP films showed lower-intermediate, and FP and SP showed low moisture barrier effects. It is important to note that the crosslinking did not cause a significant change in the WVP of films obtained from CP and AP ($p > 0.05$). In contrast, FP, SP, and PSP films showed 1.7-2-fold higher WVP than their respective crosslinked films ($p < 0.05$). These results suggested that the crosslinking caused formation of denser morphologies for fig pectin films. The WVP values reported in the literature suggested that all pristine fig pectin films developed in the current work showed greater moisture barrier effects than pristine orange and mango peel pectin films (64.7-76.56 $g.mm.m^{-2}.day^{-1}.kPa^{-1}$) (Spatafora Salazar et al., 2019), apple pectin film prepared with pomegranate juice (72 $g.mm.m^{-2}.day^{-1}.kPa^{-1}$) (Azeredo et al., 2016), pomegranate peel pectin film (60.48 $g.mm.m^{-2}.day^{-1}.kPa^{-1}$) (Oliveira et al., 2016). Pristine pumpkin pectin film (22.2 $g.mm.m^{-2}.day^{-1}.kPa^{-1}$) (Lalnunthari et al., 2020), lime peel pectin film (16.07 $g.mm.m^{-2}.day^{-1}.kPa^{-1}$) (Rodsamran & Sothornvit, 2019a), and lemon waste pectin-sweet potato starch blend film (23.76 $g.mm.m^{-2}.day^{-1}.kPa^{-1}$) (Dash et al., 2019) showed

409 better moisture barrier effect than pristine FP and SP pectin films, but lower moisture barrier
410 effect than PSP pectin films.

411 The Pearson's coefficient of correlations (r) suggested that there are significant negative
412 correlations between WVP of pristine films and GA content (r= -0.770) and DE (r= -0.846) of
413 pectins used for film making. These findings suggested that pristine films with good moisture
414 barrier properties need the use of high homogalacturonan pectins with a high degree of
415 esterification. This result supported the recent finding of Huang et al. (2021), who showed that
416 hydrophobic methyl ester groups in pectins are crucial for the moisture barrier effect of their
417 films. On the other hand, the WVPs of crosslinked films showed a significant negative
418 correlation with DA (r=-0.862) of pectins used in film-making. In the literature, it was reported
419 that the high degree of acetylation interfered with the gelation of pectins since the presence of
420 acetyl groups caused steric hindrance for chain association (Vriesmann & Petkowicz
421 2013). However, it appears that the steric hindrance caused in hydrated pectin molecules by
422 acetyl groups worked differently in dry films. It is well known that the increased degree of
423 acetylation causes a parallel increase in the hydrophobicity of hydrocolloids such as pectin and
424 cellulose since this replaces hydrophilic groups/bonds with hydrophobic acetyl groups (Leroux
425 et al., 2003; Ouarhim et al., 2019). The data in the literature about the effect of acetyl groups in
426 pectins on the WVP of their films are scarce. However, the current work showed for the first
427 time that acetyl groups of fig pectins (DA changed between 7 and 30%) are highly effective on
428 the WVP of their films when these pectins were crosslinked to form an "egg-box model"
429 configuration. Moreover, it is also important to note that the DA of pectins correlated
430 significantly with their TPC (r=0.884). The hydrophobic interactions formed between aromatic
431 rings (e.g., A and C rings of flavonoids) of polyphenols and hydrophobic methyl groups of
432 pectin are accepted as the primary mechanism of polyphenol-pectin complexation (Tang et al.

433 2003, Liu et al. 2020). Thus, further studies are needed to understand possible hydrophobic
434 interactions between polyphenols and acetyl groups of pectins.

435 **3.5. Oxygen barrier properties**

436 The oxygen permeability coefficients ($P'O_2$) of pectin films are reported in Table 3. The
437 best oxygen barrier performance among pristine films was observed for CP film (10776
438 $mL.\mu m.m^{-2}.24h^{-1}.atm^{-1}$), followed by AP and PSP films with 1.4 and 1.5-fold higher, and by SP
439 and FP films with almost 2.6- and 4.7-fold higher $P'O_2$s than CP film, respectively. The
440 crosslinking significantly reduced the P′O2 of all films ($p<0.05$). However, the most dramatic
441 reductions in $P'O_2$s of pristine films by crosslinking occurred for those of SP and FP films (5.2
442 and 3.7-fold), while crosslinking caused considerably smaller reductions in $P'O_2$s of PSP, CP,
443 and AP films (1.2 to 1.4-fold). These results suggested dramatic changes in molecular
444 interactions and/or morphologies in the film matrix of pristine SP and FP films by crosslinking.
445 The SP-Ca^{++} film with a $P'O_2$ of 8265 $mL.\mu m.m^{-2}.24h^{-1}.atm^{-1}$ showed the highest oxygen barrier
446 effect among the crosslinked films, followed by CP-Ca^{++} film with 1.5-fold higher, and PSP-
447 Ca^{++}, AP-Ca^{++} and FP-Ca^{++} films with 2.1 to 2.5-fold higher $P'O_2$s than that of SP-Ca^{++} film.
448 Interestingly, the SP film showed almost 1.8-fold higher $P'O_2$ than PSP film, while SP-Ca^{++}
449 film showed almost 2-fold lower $P'O_2$ than PSP-Ca^{++} film. These results clearly showed that
450 the films of crude and purified stalk waste pectins showed considerably different oxygen barrier
451 mechanisms in pristine and crosslinked forms. It appears that the loss of low methoxyl pectin
452 factions in PSP by purification is the main reason for limited changes in $P'O_2$ of its crosslinked
453 film.

454 The Pearson's coefficient of correlations (r) showed that there are significant negative
455 correlations between $P'O_2$ of pristine films and DE (r= -0.823), GA (r= -0.772), and R1 (r= -
456 0.743) of pectins used for film making. Thus, it is clear that the oxygen barrier properties of
457 pristine films depend on the amount of linear galacturonic acid units having high degree of

methylation. This finding clearly explains the lower $P'O_2$ of pristine PSP film than pristine SP film. There is also a significant positive correlation between the soluble protein content of pectins and the $P'O_2$ of their pristine films. This finding indicates that the soluble proteins distributed within the pectin film matrix spoiled (defected) the desired homogalacturonan film network formed by entangled linear pectin molecules. In contrast, there were no significant correlations between investigated pectin molecular and compositional parameters and $P'O_2$ of crosslinked films. Thus, it seemed that the oxygen gas barrier effect of crosslinked films is simply a result of formed dense morphology (increased film networking) by the formation of an ordered egg-box structure. Further studies are needed to understand the oxygen barrier properties of crosslinked pectin films.

3.6. Solubility and swelling of pectin films

The solubilities of pectin films are shown in Fig. 1. The pristine films of CP, AP, and PSP showed 100% solubility, while pristine FP and SP films showed almost 71-72% solubility due possibly to the crude nature of their pectins. The crosslinking caused a significant reduction in the solubility of films obtained from CP, SP, and FP. Thus, the lowest solubility was obtained for FP-Ca^{++} (32.8%) followed by SP-Ca^{++} (38.6%) and CP-Ca^{++} (41.8%). This result clearly showed that the CP, SP, and FP pectin contained a considerable amount of low methoxyl pectin (LMP) fractions necessary for sufficient crosslinking of films by the Ca^{++} ions due to the formation of the "egg-box model". In contrast, AP-Ca^{++} and PSP-Ca^{++} showed 100% and 76% solubilities, respectively. The limited reduction in solubility of PSP-Ca^{++} by crosslinking once more suggested that the purification of SP removed mainly the LMP fractions of PSP pectin. The Pearson's coefficient of correlations (r) suggested that there are significant positive correlations between water solubility of pristine films and GA (r=0.778), DE (r=0.824), and R1 (r=0.805) of pectins. However, the only significant correlation for crosslinked films was determined between the solubility of these films and the DE of pectins (r=0.804) used in film

483 making. This finding clearly showed that the DE of pectins is a very critical factor affecting the
484 solubility of both pristine and crosslinked films.

485 Due to the high solubility of pristine films, the swelling properties were determined only
486 for the crosslinked films except for AP-$Ca^{++,}$ which showed 100% solubility (Fig 1). The
487 highest degree of swelling was observed for CP-$Ca^{++,}$ followed in descending order by PSP-
488 Ca^{++}, SP-$Ca^{++,}$ and FP-Ca^{++} films that showed almost 1.9, 2.4, and 3.2-fold less swelling than
489 CP-Ca^{++} film, respectively. Therefore, it is clear that the FP-Ca^{++} films were not only the least
490 soluble films but also the least swellable films. Due to the limited number of films used in this
491 test, no regression analysis was conducted for film swelling.

492 **3.7. Surface wettability of pectin films**

493 The water contact angles and contact moment images of pectin films are given in Fig.3
494 and Fig.4-A to J), respectively. The film surface could act as completely wettable (hydrophilic),
495 partially wettable, or not wettable (hydrophobic) by the solvent when the contact angle is
496 measured at <30º, between 30º and 90º, and >90º, respectively (Chaiwarit et al., 2020). The
497 contact angles of pristine and crosslinked pectin films varied between 41 and 80º, 48 and 102º,
498 respectively. None of the pectin films showed complete wettability, but the majority of films
499 are distributed mainly at the lower and higher limits of the partially wettable category, with the
500 exception of FP-Ca^{++} that was identified as the only not wettable film under the test conditions.
501 This result complies well with previous findings that showed the greatest resistance of FP-Ca^{++}
502 films against solubility and swelling. The ranking of the hydrophobicities of pristine film
503 surfaces in decreasing order was as follows; AP, FP, PSP, SP, and CP. Interestingly, the
504 wettability values of pristine fig pectin films varied between those of two commercial pectin
505 films. The crosslinking caused significant changes in hydrophilic/hydrophobic properties of all
506 films ($P>0.05$). For example, CP-Ca++, FP-Ca++, and SP-Ca++ films turned more hydrophobic
507 (1.3-1.4-fold higher θ values) than their respective pristine films (CP, FP, SP films) by

crosslinking. This finding clearly explained the low solubility of CP-Ca^{++}, FP-$Ca^{++,}$ and SP-Ca^{++} films in distilled water. In contrast, AP-Ca^{++} and PSP-Ca^{++} films showed slightly higher hydrophilicity than their respective pristine films (AP and PSP films). Thus, the overall ranking of crosslinked film surface hydrophobicity in decreasing order was as follows; FP-Ca^{++}, AP-Ca^{++}, SP-Ca^{++}, CP-Ca^{++}, and PSP-Ca^{++}.

The analysis of Pearson's coefficient of correlations suggests that there was a moderate negative correlation (r= -0.773) between the GA content of pectins and the water contact angle of crosslinked films. This finding suggests that the hydrophilic groups of homogalacturonan units play a central role in determining crosslinked film surface hydrophilicity. In contrast, no significant correlations were determined between water contact angles of pristine films and molecular and compositional parameters of pectins used in film-making.

3.8. Morphology of pectin films

The morphologies of films were investigated by AFM and SEM. The surface morphologies (Fig. 5A-J) and topographic images (Fig. 6A-J) of films obtained by AFM clearly showed the rough surfaces of all pectin films. The Rrms and Rmax of pectin films varied at a broad range between 7.65 and 31.9 nm and 59.9 and 224 nm, respectively (Table 4). Considering the roughness parameters, the PSP-Ca^{++} showed the highest roughness followed in descending order by PSP and SP films that also showed considerable roughness, and SP-Ca^{++}, CP-Ca^{++}, CP, FP films with intermediate roughness, and FP-Ca^{++}, AP, AP-Ca^{++} films with limited roughness. The crosslinking caused some different effects on the surface roughness of pectin films. For example, Rrms values of pristine and crosslinked films of AP, SP, and PSP pectins were similar, while crosslinking caused a significant increase and reduction in Rrms values of films obtained from CP and FP pectins, respectively. Moreover, pristine and crosslinked films of CP, AP, and FP pectins showed similar Rmax values, while crosslinking caused an increase and reduction of Rmax values for films obtained from PSP and SP pectins,

respectively. It is interesting to note that the AP films were the only ones not to be affected by crosslinking.

Fig 7A to 7J show the SEM micrographs of film surfaces at 500× magnification. The surfaces of pristine and crosslinked films from commercial pectins and SP pectin were smooth and homogeneous, and they were apparenlty free from pores, cracks, and air bubbles. The SEM micrographs also proved that the PSP film surface was rough, but it was also evident that these films too were apparenlty free from pores and cracks. In contrast, extensive tiny craters were clearly identifiable on both pristine and crosslinked FP film surfaces (Fig.7C and 7H). The crosslinking improved the surface smoothness of films obtained from commercial pectins and SP pectin, but no apparent changes were observed in the surface morphologies of FP and PSP films by crosslinking. Figure 8A to 8J also shows the cross-sectional SEM images of different pectin films at 2500× magnification. The comparison of cross-sectional images of pristine and crosslinked films indicated that the crosslinking caused formation of extensive networking (intensive tiny aggregations) within films. Some heterogeneous formations were observed in FP-Ca^{++}, SP-Ca^{++} and PSP-Ca^{++}, but CP-Ca^{++} and AP-Ca^{++} showed more homogeneous cross-sectional images. No apparent pores and cracks were identified at film cross-sections, except those of FP and FP-Ca^{++} films that contained some burst spherical void capsules concentrated mainly at the upper part of the film surface. The FP pectin showed the highest soluble protein content thus, these spherical formations might be formed by protein stabilized tiny air bubbles. These results showed that the morphology of all films changed to some extent by crosslinking. Thus, it appears that the changes in surface roughness and internal morphology together with molecular and compositional parameters determined the final mechanical and barrier properties of crosslinked pectin films. This finding also suggests that properties of crosslinked films that lack to show any correlation with molecular and compositional parameters of pectins are affected mainly by morphological changes induced by egg box model formation. For example,

the $P'O_2$ of crosslinked films that lacked to show any correlations with parameters measured for pectin might be related mainly to changes in film morphology. Further studies are needed to determine the exact contribution of morphology to mechanical and barrier properties of pectin films.

3.9. Transparency and color of pectin films

The transparency values (%) of pristine films ranged between 13.8 and 27.2% (Table 5). The AP gave the most transparent pristine film followed by pristine films of CP and SP with intermediate transparency and pristine films of PSP and FP with low transparency. In all pristine films, the crosslinking caused a significant increase in film transparency ($p<0.05$). The transparency of crosslinked films ranged between 15.8 and 32.6%, but the transparency ranking for the crosslinked films is similar to that of pristine films. According to Hong et al. (2005), the transparency values of polypropylene and low-density polyethylene (LDPE) films were almost 38% and 15–20%, respectively. Thus, it appears that the transparencies of pectin films are comparable to those of LDPP films. It is important to note that SP and SP-Ca^{++} films showed significantly greater transparency values than PSP and PSP-Ca^{++} films. This finding clearly showed that the purification of fig stalk waste pectin did not result in increased film transparency. In general, the film transparency is determined by morphology rather than chemical composition (Farris et al 2009). Thus, it seemed that the difference between the transparency of crude and purified stalk waste pectin films originated from significant differences between their surface (Rrms or Rmax) and cross-sectional morphologies.

The color of films evaluated considering lightness (L*), yellowness (a*), and redness (b*) values and photos of films were given in Table 5 and Fig. 9, respectively. The L* values of films changed between 66.3 and 85.8. The crosslinking did not cause a considerable change in the L* value of films except CP which showed a slight increase in L* by crosslinking. The AP and CP gave the lightest colored films (Fig 9A-D), while all fig pectin films were dark-

583 colored (Fig. 9E-J) due to the Maillard reaction products that formed a tight complex with the
584 extracted pectins. However, it must be noted that the purified PSP contained less Maillard
585 reaction products, thus, it gave lighter films than SP that is a crude stalk waste pectin. The
586 pristine fig pectin films also showed significantly higher a* values than pristine commercial
587 pectin films ($p < 0.05$). The crosslinking increased the a* values of films except for pristine PSP
588 films that showed similar a* with PSP-Ca^{++} films. The b* values of fig pectin films were
589 comparable with those of CP films, while AP showed considerably lower b* values than all
590 pectin films.

591 **4. Conclusions**

592 This work clearly showed the potential advantages of using pectins extracted from stalk
593 waste of processed high-quality figs in the development of edible films. Edible films of purified
594 stalk waste pectin showed superior mechanical strength than commercial apple pectin, while
595 having comparable mechanical strength with commercial citrus pectin. The pristine and
596 crosslinked films of purified stalk waste pectin had the highest moisture barrier effects, while
597 crosslinked crude stalk waste pectin film showed the highest oxygen gas barrier effect. The
598 films of pectin extracted from low-grade substandard fig fruits did not show outstanding
599 mechanical and barrier properties, but the cross-linked films of this pectin showed the highest
600 surface hydrophobicity, and lowest solubility and swelling. The analysis of Pearson's
601 coefficient of correlations revealed fundamental knowledge about the effects of molecular and
602 compositional parameters of studied pectins on the properties of their pristine and $CaCl_2$
603 crosslinked films. The major findings are as follows: (1) galacturonic acid content of pectins is
604 the primary factor correlating positively with mechanical strength and stiffness of pristine and
605 crosslinked films, (2) a significant positive correlation exists between RG-I content of pectins
606 and flexibility of pristine and crosslinked films, (3) moisture barrier effect of pristine films
607 correlates with high galacturonic acid content and high degree of esterification while moisture

barrier effect of cross-linked films correlates with high degree of acetylation, (4) oxygen barrier effect of pristine films correlates with the amount of linear galacturonic acid units having high degree of methylation. This work not only introduced fig stalk pectin as an alternative hydrocolloid that gives some superior edible film characteristics than commercial pectins, but also it expands the fundamental knowledge about factors affecting the mechanical and barrier properties of pectin films.

CRediT authorship contribution statement

Elif Çavdaroğlu: Conceptualization, Investigation, Methodology, Data curation, Writing – original draft. **Stefano Farris:** Conceptualization, Methodology, Writing – review & editing. **Ahmet Yemenicioğlu:** Conceptualization, Methodology, Supervision, Project administration, Writing – review & editing.

Acknowledgments

This work is part of the Ph.D. thesis of author Elif Çavdaroğlu, and it was funded by The Scientific and Technical Research Council of Turkey (TÜBİTAK, Project no: 118 O 372). We thank Integrated Research Center at Izmir Institute of Technology for AFM and SEM analyses. Additionally, we thank Assoc. Prof. Dr. Ali Oğuz Büyükkileci for his guidance through the HPLC analysis. We thank Duygu Büyüktaş for her help in OTR measurements. Prof. Dr. Stefano Farris contributed to surface wettability and OTR measurements while other experimental parts were conducted by the Ph.D. student Elif Çavdaroğlu.

Ethical guidelines

Ethics approval was not required for this research.

Data availability statement

631 Research data are not shared.

632 **Conflict of interest**

633 There are no conflicts of interest in this study.

634

635 **References**

636 Alba, K., & Kontogiorgos, V. (2017). Pectin at the oil-water interface: Relationship of
637 molecular composition and structure to functionality. *Food Hydrocolloids*, *68*, 211–218.
638 https://doi.org/10.1016/j.foodhyd.2016.07.026

639 Anonymous. (2021). Nuts an dried fruits statistical yearbook 2020/2021. In *International Nut*
640 *and Dried Fruit Council*.

641 AOAC. (1990). In *Official methods of analysis (15th ed.). Washington, DC: Association of*
642 *Official Analytical Chemists.*

643 ASTM. (2002a). Standard test method for tensile properties of thin plastic sheeting- D882-02.
644 In *Annual Book of American Standard Testing Methods* (Vol. 14).

645 ASTM. (2002b). Standard Test Method for Transparency of Plastic Sheeting-D 1746-97. In
646 *Annual Book of American Standard Testing Methods* (Vol. 8).
647 https://doi.org/10.1520/C1530_C1530M-04R10E01.

648 ASTM. (2016). Standard Test Methods for Water Vapor Transmission of Materials E96/E96M.
649 In *Annual Book of ASTM Standards: Vol. i*. https://doi.org/10.1520/E0096_E0096M-16

650 Azeredo, H. M. C., Morrugares-Carmona, R., Wellner, N., Cross, K., Bajka, B., & Waldron, K.
651 W. (2016). Development of pectin films with pomegranate juice and citric acid. *Food*
652 *Chemistry*, *198*, 101–106. https://doi.org/10.1016/j.foodchem.2015.10.117

653 Basak, S., & Annapure, U. S. (2022). Trends in "green" and novel methods of pectin
654 modification - A review. *Carbohydrate Polymers*, *278*(November 2021), 118967.
655 https://doi.org/10.1016/j.carbpol.2021.118967

656 Blumenkrantz, N., & Asboe-Hansen, G. (1973). New method for quantitative determination of
657 uronic acids. *Analytical Biochemistry*, *54*(2), 484–489. https://doi.org/10.1016/0003-

2697(73)90377-1

Bradford, M. M. (1976). A dye binding assay for protein. *Anal. Biochem.*, *72*, 248–254.

Broxterman, S. E., Picouet, P., & Schols, H. A. (2017). Acetylated pectins in raw and heat processed carrots. *Carbohydrate Polymers*, *177*(August), 58–66. https://doi.org/10.1016/j.carbpol.2017.08.118

Çavdaroğlu, E., Farris, S., & Yemenicioğlu, A. (2020). Development of pectin–eugenol emulsion coatings for inhibition of Listeria on webbed-rind melons: a comparative study with fig and citrus pectins. *International Journal of Food Science & Technology*, *55*(4), 1448–1457. https://doi.org/10.1111/ijfs.14458

Çavdaroğlu, E., & Yemenicioğlu, A. (2022). Utilization of stalk waste separated during processing of sun-dried figs (Ficus carica) as a source of pectin: Extraction and determination of molecular and functional properties. *LWT*, *154*, 112624. https://doi.org/10.1016/j.lwt.2021.112624

Chaiwarit, T., Masavang, S., Mahe, J., Sommano, S., Ruksiriwanich, W., Brachais, C. H., Chambin, O., & Jantrawut, P. (2020). Mango (cv. Nam Dokmai) peel as a source of pectin and its potential use as a film-forming polymer. *Food Hydrocolloids*, *102*(December 2019). https://doi.org/10.1016/j.foodhyd.2019.105611

Chandrayan, P. (2018). Biological Function(s) and Application (s) of Pectin and Pectin Degrading Enzymes. *Biosciences, Biotechnology Research Asia*, *15*(1), 87–100. https://doi.org/10.13005/bbra/2611

Dash, K. K., Ali, N. A., Das, D., & Mohanta, D. (2019). Thorough evaluation of sweet potato starch and lemon-waste pectin based-edible films with nano-titania inclusions for food packaging applications. *International Journal of Biological Macromolecules*, *139*, 449–

458. https://doi.org/10.1016/j.ijbiomac.2019.07.193

Denman, L. J., & Morris, G. A. (2015). An experimental design approach to the chemical characterisation of pectin polysaccharides extracted from Cucumis melo Inodorus. *Carbohydrate Polymers*, *117*, 364–369. https://doi.org/10.1016/j.carbpol.2014.09.081

Dranca, F., & Oroian, M. (2018). Extraction, purification and characterization of pectin from alternative sources with potential technological applications. *Food Research International*, *113*(June), 327–350. https://doi.org/10.1016/j.foodres.2018.06.065

Dubois, M., Gilles, K. A., Hamilton, J. K., Rebers, Pa. A., & Smith, F. (1956). Colorimetric Method for Determination of Sugars and Related Substances. *Analytical Chemistry*, *28*(3), 350–356. https://doi.org/10.1021/ac60111a017

Farris, S., Introzzi, L., & Piergiovanni, L. (2009). Evaluation of a bio-coating as a solution to improve barrier, friction and optical properties of plastic films. *Packaging Technology and Science*, *22*(2), 69–83. https://doi.org/10.1002/pts.826

Fraeye, I., Doungla, E., Duvetter, T., Moldenaers, P., Van Loey, A., & Hendrickx, M. (2009). Influence of intrinsic and extrinsic factors on rheology of pectin-calcium gels. *Food Hydrocolloids*, *23*(8), 2069–2077. https://doi.org/10.1016/j.foodhyd.2009.03.022

Gamonpilas, C., Buathongjan, C., Kirdsawasd, T., Rattanaprasert, M., Klomtun, M., Phonsatta, N., & Methacanon, P. (2021). Pomelo pectin and fiber: Some perspectives and applications in food industry. *Food Hydrocolloids*, *120*(April), 106981. https://doi.org/10.1016/j.foodhyd.2021.106981

Gharibzahedi, S. M. T., Smith, B., & Guo, Y. (2019a). Pectin extraction from common fig skin by different methods: The physicochemical, rheological, functional, and structural evaluations. *International Journal of Biological Macromolecules*, *136*, 275–283. https://doi.org/10.1016/j.ijbiomac.2019.06.040

706 Gharibzahedi, S. M. T., Smith, B., & Guo, Y. (2019b). Ultrasound-microwave assisted
707 extraction of pectin from fig (Ficus carica L.) skin: Optimization, characterization and
708 bioactivity. *Carbohydrate Polymers*, *222*(April), 114992.
709 https://doi.org/10.1016/j.carbpol.2019.114992

710 Gilani, A. H., Mehmood, M. H., Janbaz, K. H., Khan, A. ullah, & Saeed, S. A. (2008).
711 Ethnopharmacological studies on antispasmodic and antiplatelet activities of Ficus carica.
712 *Journal of Ethnopharmacology*, *119*(1), 1–5. https://doi.org/10.1016/j.jep.2008.05.040

713 Henao-Díaz, L. S., Cadena-Casanova, C. L., Bolio López, G. I., Veleva, L., Azamar-Barrios, J.
714 A., Hernández-Villegas, M. M., & Córdova-Sánchez, S. (2021). Obtaining and
715 characterization films of a bioplastic obtained from passion fruit waste (Passiflora edulis).
716 *Agro Productividad*, *II*. https://doi.org/10.32854/agrop.v14i7.2010

717 Houben, K., Jolie, R. P., Fraeye, I., Van Loey, A. M., & Hendrickx, M. E. (2011). Comparative
718 study of the cell wall composition of broccoli, carrot, and tomato: Structural
719 characterization of the extractable pectins and hemicelluloses. *Carbohydrate Research*,
720 *346*(9), 1105–1111. https://doi.org/10.1016/j.carres.2011.04.014

721 Jakobek, L. (2015). Interactions of polyphenols with carbohydrates, lipids and proteins. *Food*
722 *Chemistry*, *175*, 556–567. https://doi.org/10.1016/j.foodchem.2014.12.013

723 Kelebek, H., Dıblan, S., Kadiroğlu, P., Kola, O., & Selli, S. (2018). Kurutma İşlemlerinin
724 İncirlerin (Ficus Carica L.) Fenolik Bileşikler, Antioksidan Kapasite ve Diğer Önemli Bazı
725 Kalite Kriterleri Üzerine Etkileri. *Çukurova Tarım Gıda Bil. Der.*, *33*(2), 127–136.

726 Lalnunthari, C., Devi, L. M., & Badwaik, L. S. (2020). Extraction of protein and pectin from
727 pumpkin industry by-products and their utilization for developing edible film. *Journal of*
728 *Food Science and Technology*, *57*(5), 1807–1816. https://doi.org/10.1007/s13197-019-
729 04214-6

730 Leroux, J., Langendorff, V., Schick, G., Vaishnav, V., & Mazoyer, J. (2003). Emulsion
731 stabilizing properties of pectin. *Food Hydrocolloids*, *17*(4), 455–462.
732 https://doi.org/10.1016/S0268-005X(03)00027-4

733 Li, L., Gao, X., Liu, J., Chitrakar, B., Wang, B., & Wang, Y. (2021). Hawthorn pectin:
734 Extraction, function and utilization. *Current Research in Food Science*, *4*(June), 429–435.
735 https://doi.org/10.1016/j.crfs.2021.06.002

736 Liu, X., Le Bourvellec, C., & Renard, C. M. G. C. (2020). Interactions between cell wall
737 polysaccharides and polyphenols: Effect of molecular internal structure. *Comprehensive*
738 *Reviews in Food Science and Food Safety*, *19*(6), 3574–3617.
739 https://doi.org/10.1111/1541-4337.12632

740 M'sakni, N. H., Majdoub, H., Roudesli, S., Picton, L., Le Cerf, D., Rihouey, C., & Morvan, C.
741 (2006). Composition, structure and solution properties of polysaccharides extracted from
742 leaves of Mesembryanthenum crystallinum. *European Polymer Journal*, *42*(4), 786–795.
743 https://doi.org/10.1016/j.eurpolymj.2005.09.014

744 Muñoz-Almagro, N., Montilla, A., & Villamiel, M. (2020). Role of pectin in the current trends
745 towards low-glycaemic food consumption. *Food Research International*, *October*,
746 109851. https://doi.org/10.1016/j.foodres.2020.109851

747 Noreen, A., Nazli, Z. i. H., Akram, J., Rasul, I., Mansha, A., Yaqoob, N., Iqbal, R., Tabasum,
748 S., Zuber, M., & Zia, K. M. (2017). Pectins functionalized biomaterials; a new viable
749 approach for biomedical applications: A review. *International Journal of Biological*
750 *Macromolecules*, *101*, 254–272. https://doi.org/10.1016/j.ijbiomac.2017.03.029

751 Oliveira, T. Í. S., Zea-Redondo, L., Moates, G. K., Wellner, N., Cross, K., Waldron, K. W., &
752 Azeredo, H. M. C. (2016). Pomegranate peel pectin films as affected by montmorillonite.
753 *Food Chemistry*, *198*, 107–112. https://doi.org/10.1016/j.foodchem.2015.09.109

Ouarhim, W., Zari, N., Bouhfid, R., & el kacem Qaiss, A. (2019). 3 - Mechanical performance of natural fibers–based thermosetting composites. In M. Jawaid, M. Thariq, & N. Saba (Eds.), *Mechanical and Physical Testing of Biocomposites, Fibre-Reinforced Composites and Hybrid Composites* (pp. 43–60). Woodhead Publishing. https://doi.org/https://doi.org/10.1016/B978-0-08-102292-4.00003-5

Pérez, L. M., Piccirilli, G. N., Delorenzi, N. J., & Verdini, R. A. (2016). Effect of different combinations of glycerol and/or trehalose on physical and structural properties of whey protein concentrate-based edible films. *Food Hydrocolloids*, *56*, 352–359. https://doi.org/10.1016/j.foodhyd.2015.12.037

Reichembach, L. H., & Lúcia de Oliveira Petkowicz, C. (2021). Pectins from alternative sources and uses beyond sweets and jellies: An overview. *Food Hydrocolloids*, *118*(April), 106824. https://doi.org/10.1016/j.foodhyd.2021.106824

Rezvanain, M., Ahmad, N., Mohd Amin, M. C. I., & Ng, S. F. (2017). Optimization, characterization, and in vitro assessment of alginate-pectin ionic crosslinked hydrogel film for wound dressing applications. *International Journal of Biological Macromolecules*, *97*, 131–140. https://doi.org/10.1016/j.ijbiomac.2016.12.079

Rodsamran, P., & Sothornvit, R. (2019a). Lime peel pectin integrated with coconut water and lime peel extract as a new bioactive film sachet to retard soybean oil oxidation. *Food Hydrocolloids*, *97*(June), 105173. https://doi.org/10.1016/j.foodhyd.2019.105173

Rodsamran, P., & Sothornvit, R. (2019b). Preparation and characterization of pectin fraction from pineapple peel as a natural plasticizer and material for biopolymer film. *Food and Bioproducts Processing*, *118*, 198–206. https://doi.org/10.1016/j.fbp.2019.09.010

Rtibi, K., Selmi, S., Grami, D., Sebai, H., & Marzouki, L. (2018). Laxative and anti-purgative bioactive compounds in prevention and treatment of functional gastrointestinal disorders,

778 constipation and diarrhea. *Journal of Nutritional Health & Food Engineering*, *8*(6), 8–10.
779 https://doi.org/10.15406/jnhfe.2018.08.00312

780 Schmidt, U. S., Koch, L., Rentschler, C., Kurz, T., Endreß, H. U., & Schuchmann, H. P. (2015).
781 Effect of Molecular Weight Reduction, Acetylation and Esterification on the
782 Emulsification Properties of Citrus Pectin. *Food Biophysics*, *10*(2), 217–227.
783 https://doi.org/10.1007/s11483-014-9380-1

784 Sengkhamparn, N., Bakx, E. J., Verhoef, R., Schols, H. A., Sajjaanantakul, T., & Voragen, A.
785 G. J. (2009). Okra pectin contains an unusual substitution of its rhamnosyl residues with
786 acetyl and alpha-linked galactosyl groups. *Carbohydrate Research*, *344*(14), 1842–1851.
787 https://doi.org/10.1016/j.carres.2008.11.022

788 Simmons, M. S. J., & Preedy, V. R. (2016). *Nutritional composition of fruit cultivars*. Academic
789 Press.

790 Spatafora Salazar, A. S., Sáenz Cavazos, P. A., Mújica Paz, H., & Valdez Fragoso, A. (2019).
791 External factors and nanoparticles effect on water vapor permeability of pectin-based
792 films. *Journal of Food Engineering*, *245*(August 2018), 73–79.
793 https://doi.org/10.1016/j.jfoodeng.2018.09.002

794 Tang, H. R., Covington, A. D., & Hancock, R. A. (2003). Structure-Activity Relationships in
795 the Hydrophobic Interactions of Polyphenols with Cellulose and Collagen. *Biopolymers*,
796 *70*(3), 403–413. https://doi.org/10.1002/bip.10499

797 Trad, M., Bourvellec, C. Le, Gaaliche, B., Renard, C. M. G. C., Mars, M., Trad, M., Bourvellec,
798 C. Le, Gaaliche, B., Renard, C. M. G. C., Trad, M., Bourvellec, C. Le, Gaaliche, B.,
799 Renard, C. M. G. C., & Mars, M. (2014). *Nutritional Compounds in Figs from the Southern*
800 *Mediterranean Region*. *2912*. https://doi.org/10.1080/10942912.2011.642447

801 Trad, M., Ginies, C., Gaaliche, B., Renard, C. M. G. C., & Mars, M. (2014). Relationship

802 between pollination and cell wall properties in common fig fruit. *Phytochemistry*, *98*, 78–
803 84. https://doi.org/10.1016/j.phytochem.2013.12.011

804 Uysal Unalan, I., Wan, C., Figiel, L., Olsson, R. T., Trabattoni, S., & Farris, S.
805 (2015). Exceptional oxygen barrier performance of pullulan nanocomposites with ultra-
806 low loading of graphene oxide. *Nanotechnology*, *26*, 275703–275713.
807 https://doi.org/10.1088/0957-4484/26/27/275703

808 UNECE. (2016). *UNECE Standard DDP-15 concerning the marketing and commercial quality*
809 *control of Dried Figs*. http://www.unece.org/trade/agr/welcome.html.

810 Voragen, A. G. J., Schols, H. A., & Pilnik, W. (1986). Determination of the degree of
811 methylation and acetylation of pectins by h.p.l.c. *Topics in Catalysis*, *1*(1), 65–70.
812 https://doi.org/10.1016/S0268-005X(86)80008-X

813 Vriesmann, L. C., & Petkowicz, C. L. O. (2013). Highly acetylated pectin from cacao pod husks
814 (Theobroma cacao L.) forms gel. *Food Hydrocolloids*, *33*(1), 58–65.
815 https://doi.org/10.1016/j.foodhyd.2013.02.010

816 Wu, Y., Chen, Z., Li, X., & Li, M. (2009). Effect of tea polyphenols on the retrogradation of
817 rice starch. *Food Research International*, *42*(2), 221–225.
818 https://doi.org/10.1016/j.foodres.2008.11.001

819 Yang, X., Guo, J. L., Ye, J. Y., Zhang, Y. X., & Wang, W. (2015). The effects of Ficus carica
820 polysaccharide on immune response and expression of some immune-related genes in
821 grass carp, Ctenopharyngodon idella. *Fish & Shellfish Immunology*, *42*(1), 132–137.
822 https://doi.org/10.1016/j.fsi.2014.10.037

823 Yapo, B. M. (2011). Rhamnogalacturonan-I: A structurally puzzling and functionally versatile
824 polysaccharide from plant cell walls and mucilages. *Polymer Reviews*, *51*(4), 391–413.
825 https://doi.org/10.1080/15583724.2011.615962

826

827 **Table 1.** Different characteristics of fig fruit and stalk waste pectins and commercial pectins.

Characteristics	CP[a,b]	AP[a,b]	FP[a,b]	SP[a,b]	PSP[a,b]
Compositions of different pectins					
Total carbohydrate	89.1 ± 13.4^{A}	83.4 ± 3.76^{A}	58.9 ± 1.47^{B}	82.0 ± 8.05^{A}	84.6 ± 7.69^{A}
Moisture content	4.18 ± 0.29^{E}	7.13 ± 0.20^{B}	9.54 ± 0.04^{A}	6.76 ± 0.11^{C}	5.06 ± 0.25^{D}
Ash	4.19 ± 0.20^{B}	4.92 ± 0.62^{B}	8.19 ± 0.01^{A}	4.61 ± 0.91^{B}	4.85 ± 0.37^{B}
Soluble protein	4.19 ± 0.96^{C}	2.87 ± 0.68^{D}	11.1 ± 0.19^{A}	4.94 ± 0.09^{BC}	5.70 ± 0.26^{B}
TPC[c]	0.59 ± 0.07^{C}	0.24 ± 0.03^{D}	1.13 ± 0.08^{B}	1.09 ± 0.05^{B}	1.82 ± 0.42^{A}
Molecular properties of different pectins					
GA	78.8 ± 7.44^{A}	50.4 ± 3.74^{C}	32.4 ± 3.95^{D}	34.3 ± 3.73^{D}	63.0 ± 4.52^{B}
DE	54.6 ± 1.46^{B}	62.9 ± 0.92^{A}	36.7 ± 3.95^{D}	45.0 ± 2.52^{C}	65.9 ± 1.89^{A}
DA	3.47 ± 0.34^{D}	2.70 ± 0.07^{D}	6.96 ± 0.82^{C}	11.57 ± 0.02^{B}	29.9 ± 3.82^{A}
D-Glc	0.22 ± 0.08^{D}	6.48 ± 0.30^{A}	6.07 ± 0.03^{B}	6.15 ± 0.52^{AB}	1.72 ± 0.09^{C}
L-Rha	0.30 ± 0.05^{C}	1.57 ± 0.26^{B}	0.52 ± 0.03^{C}	2.13 ± 0.26^{A}	1.66 ± 0.40^{AB}
D-Gal	4.05 ± 0.33^{B}	1.54 ± 0.44^{C}	5.20 ± 0.46^{AB}	3.93 ± 0.65^{B}	6.26 ± 0.73^{A}
L-Ara	3.78 ± 0.72^{A}	1.84 ± 0.37^{B}	5.07 ± 0.06^{A}	4.12 ± 0.07^{A}	4.92 ± 0.43^{A}
R-1[d]	8.29	9.62	2.55	2.88	4.22
R-2	0.004	0.037	0.021	0.074	0.032
R-3	26.13	2.12	19.01	4.21	6.78
R-4	12.33	0.84	8.73	1.75	3.48

828 [a] Values are shown as mean ± standard deviation. Values at each row indicated by different
829 letters are significantly different ($p \leq 0.05$).

830 [b] All values are expressed as % on a dry basis of pectin powder except moisture content.

831 [c] TPC=total phenolic content as g GAE/ 100 g.

832

833

834

835

836 **Table 2.** Mechanical properties of pectin films.

Sample	Thickness (μm)	Tensile Strength (MPa)	Elongation at break (%)	Young's modulus (MPa)
CP	87.81 ± 2.04^{A}	17.59 ± 2.50^{B}	4.18 ± 1.74^{F}	7.56 ± 0.87^{BC}
AP	71.28 ± 0.13^{D}	6.29 ± 0.31^{E}	21.92 ± 7.70^{AB}	0.52 ± 0.12^{F}
FP	89.02 ± 11.71^{A}	3.11 ± 0.36^{F}	15.19 ± 1.23^{BC}	0.55 ± 0.05^{F}
SP	84.11 ± 1.94^{AB}	6.50 ± 1.71^{DE}	26.17 ± 0.77^{A}	0.70 ± 0.12^{F}
PSP	85.83 ± 3.61^{A}	15.58 ± 1.02^{B}	8.83 ± 1.37^{D}	5.69 ± 1.18^{C}
CP-Ca^{++}	74.70 ± 3.20^{CD}	27.66 ± 2.56^{A}	3.51 ± 0.53^{F}	11.92 ± 1.42^{A}
AP-Ca^{++}	59.57 ± 7.41^{E}	8.40 ± 2.77^{C}	5.87 ± 1.00^{E}	2.77 ± 0.47^{D}
FP-Ca^{++}	71.22 ± 1.36^{D}	5.34 ± 0.06^{E}	7.88 ± 1.61^{DE}	1.54 ± 0.27^{E}
SP-Ca^{++}	71.89 ± 5.81^{D}	7.84 ± 1.23^{CD}	14.28 ± 5.51^{C}	1.55 ± 0.33^{E}
PSP-Ca^{++}	78.37 ± 1.56^{BC}	19.14 ± 2.52^{B}	4.19 ± 1.34^{F}	8.72 ± 0.52^{AB}

837 *Data are shown as mean ± standard deviation. Data at each column indicated by different
838 letters are significantly different ($p \leq 0.05$).

839

840

841

842

843

844

845

846

847 **Table 3.** Water vapor permeability (WVP), oxygen transmission rate (OTR), and permeability
848 coefficient ($P'O_2$), and thickness values of pectin films.

Film	WVP ($g.mm.m^{-2}.day^{-1}.kPa^{-1}$)	OTR ($mL.m^{-2}.24h^{-1}$)	$P'O_2$ ($mL.\mu m.m^{-2}.24h^{-1}.atm^{-1}$)	Thickness (μm)
CP	19.12 ± 1.77^{BC}	138.16 ± 11.8^{E}	10776.4 ± 922.8^{E}	78.2 ± 3.4^{CDE}
AP	21.43 ± 6.34^{B}	204.5 ± 9.6^{C}	15460.2 ± 725.8^{C}	75.6 ± 3.5^{DE}
FP	30.39 ± 5.39^{A}	427.1 ± 25.2^{A}	51153.6 ± 3016.4^{A}	119.7 ± 26.1^{A}
SP	31.74 ± 1.42^{A}	263.6 ± 19.7^{B}	27843.5 ± 2080.3^{B}	105.6 ± 4.7^{AB}
PSP	12.85 ± 1.24^{D}	173.44 ± 18.9^{D}	15783.04 ± 201.6^{C}	91 ± 4.5^{BC}
CP-Ca^{++}	14.96 ± 3.38^{CD}	116.9 ± 6.4^{E}	8264.8 ± 452.5^{F}	70.7 ± 2.5^{DE}
AP-Ca^{++}	20.31 ± 3.46^{B}	181.8 ± 6.7^{CD}	12657.4 ± 442.9^{DE}	66.1 ± 2.6^{E}
FP-Ca^{++}	17.45 ± 4.55^{BCD}	170.60 ± 20.3^{D}	13648.24 ± 1854.4^{CD}	80.3 ± 2.87^{CDE}
SP-Ca^{++}	18.11 ± 2.84^{BC}	58.22 ± 6.7^{F}	5402.82 ± 308.3^{G}	92.8 ± 3.7^{BC}
PSP-Ca^{++}	6.28 ± 0.57^{E}	134.03 ± 15.2^{E}	11124.16 ± 1261.9^{E}	83 ± 3.2^{CD}

849 *Data are shown as mean ± standard deviation. Data at each column indicated by different
850 letters are significantly different ($p \leq 0.05$).

851

852

853

854

855

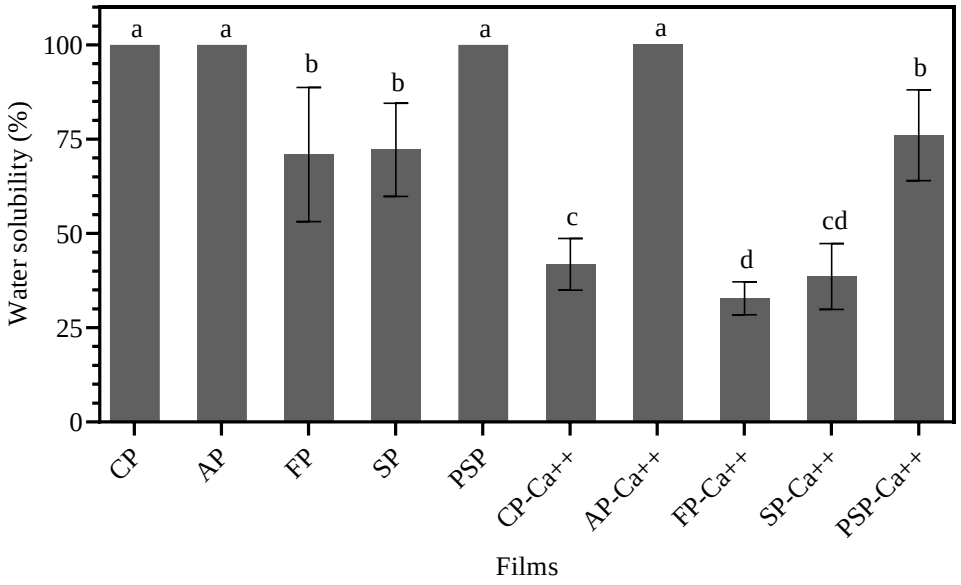

856

857 **Figure 1.** Water solubility of pectin films.

858

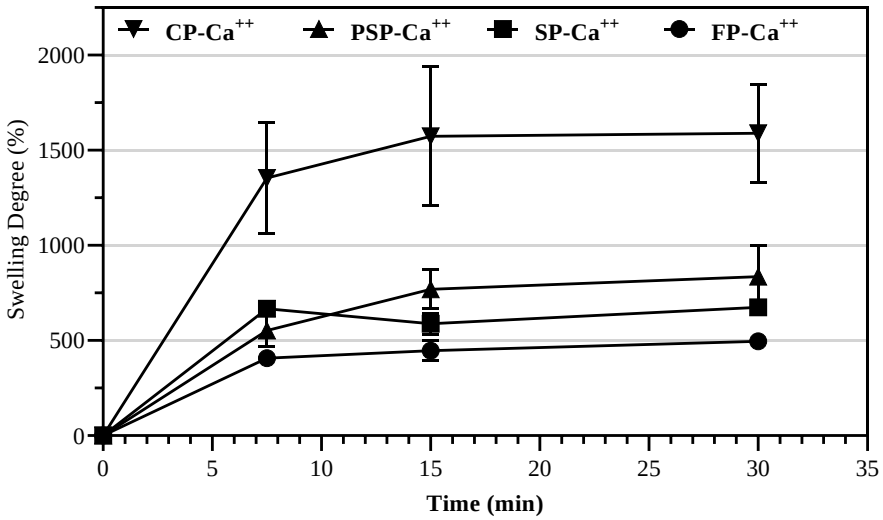

859

860 **Figure 2.** Swelling curves of pectin films.

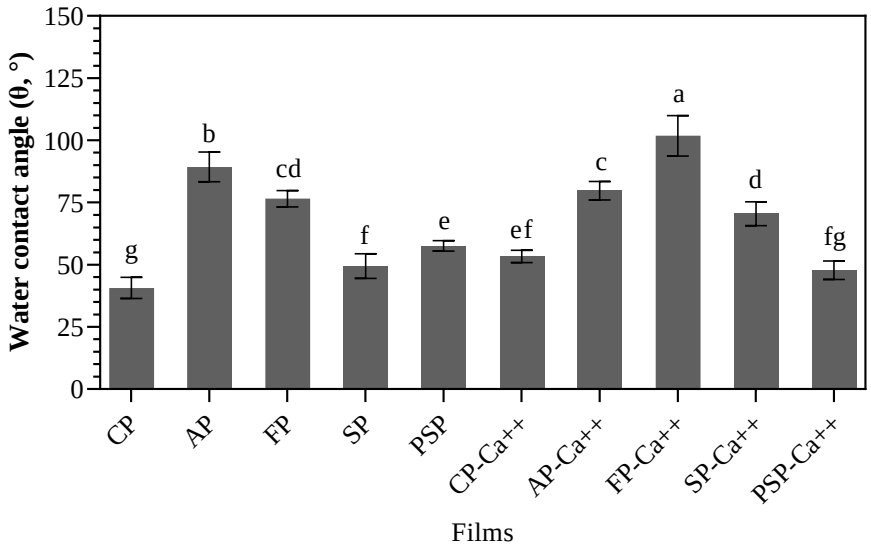

Figure 3. Water contact angle of pectin films.

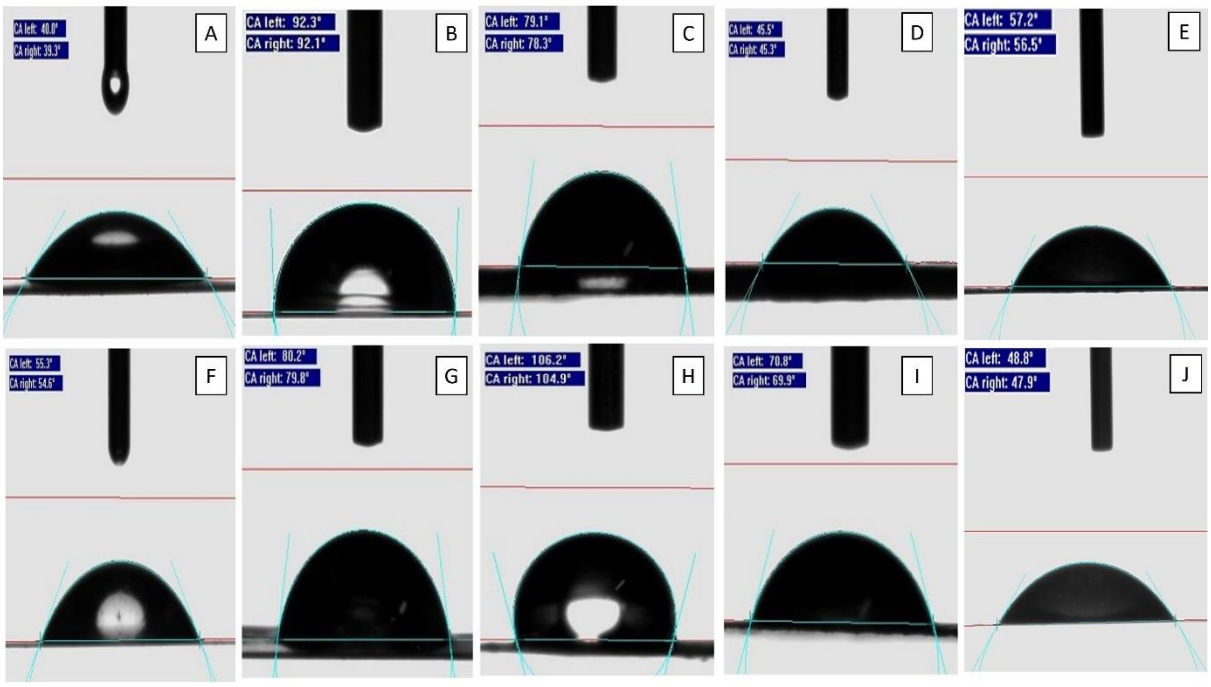

Figure 4. Instantaneous images captured at the contact between the water droplet and the

surface of pectin films: A) CP, B) AP, C) FP, D) SP, E) PSP, F) CP-Ca^{++}; (G) AP-Ca^{++}; (H) FP-Ca^{++}; (I) SP-Ca^{++}; and J) PSP-Ca^{++}.

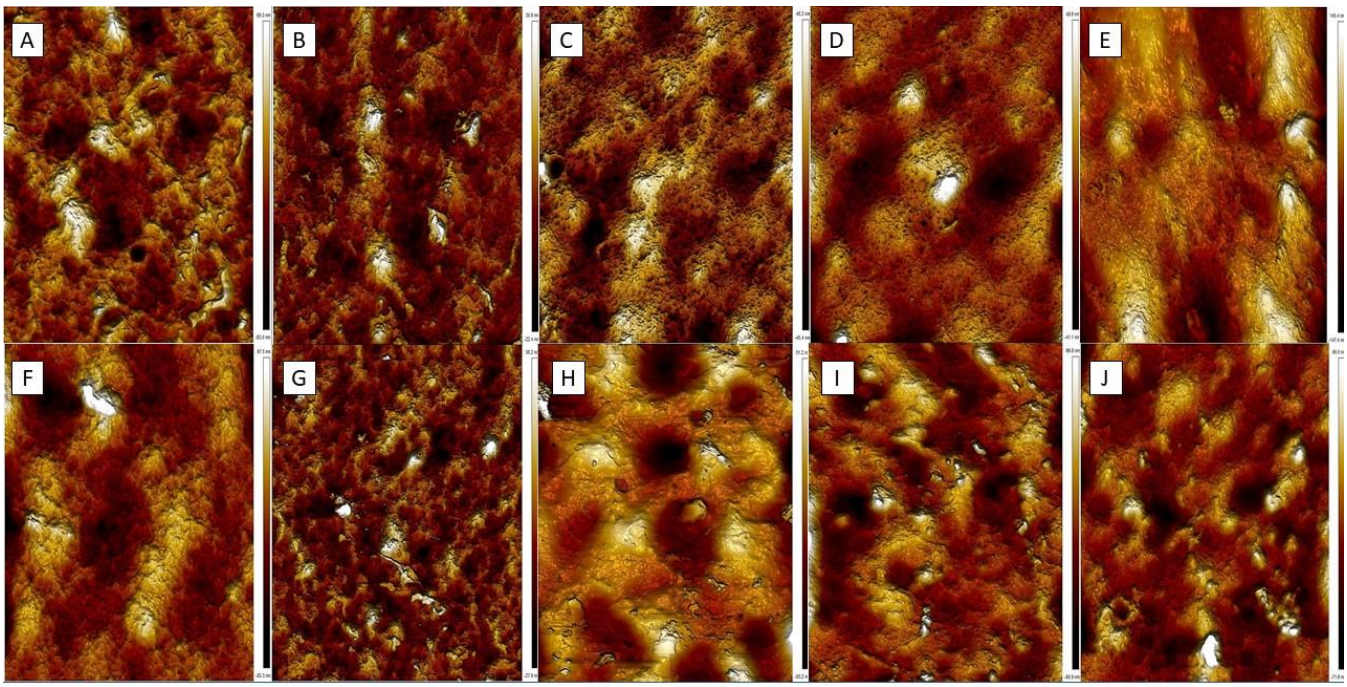

Figure 5. Surface morphologies of pectin films: (A) CP; (B) AP; (C) FP; (D) SP; E) PSP; (F) CP-Ca^{++}; (G) AP-Ca^{++}; (H) FP-Ca^{++}; (I) SP-Ca^{++}; and J) PSP-Ca^{++}.

878

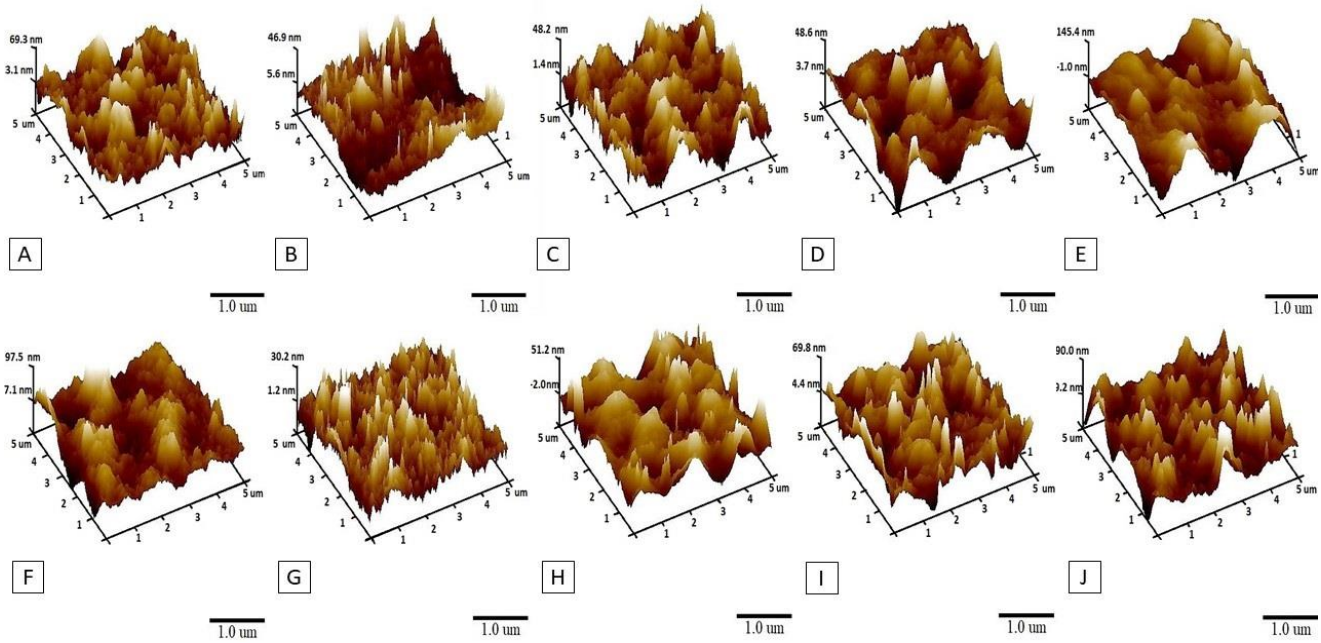

879

880 **Figure 6.** Topographic images of pectin films: (A) CP; (B) AP; (C) FP; (D) SP; E) PSP; (F)

881 CP-Ca^{++}; (G) AP-Ca^{++}; (H) FP-Ca^{++}; (I) SP-Ca^{++}; and J) PSP-Ca^{++}.

882

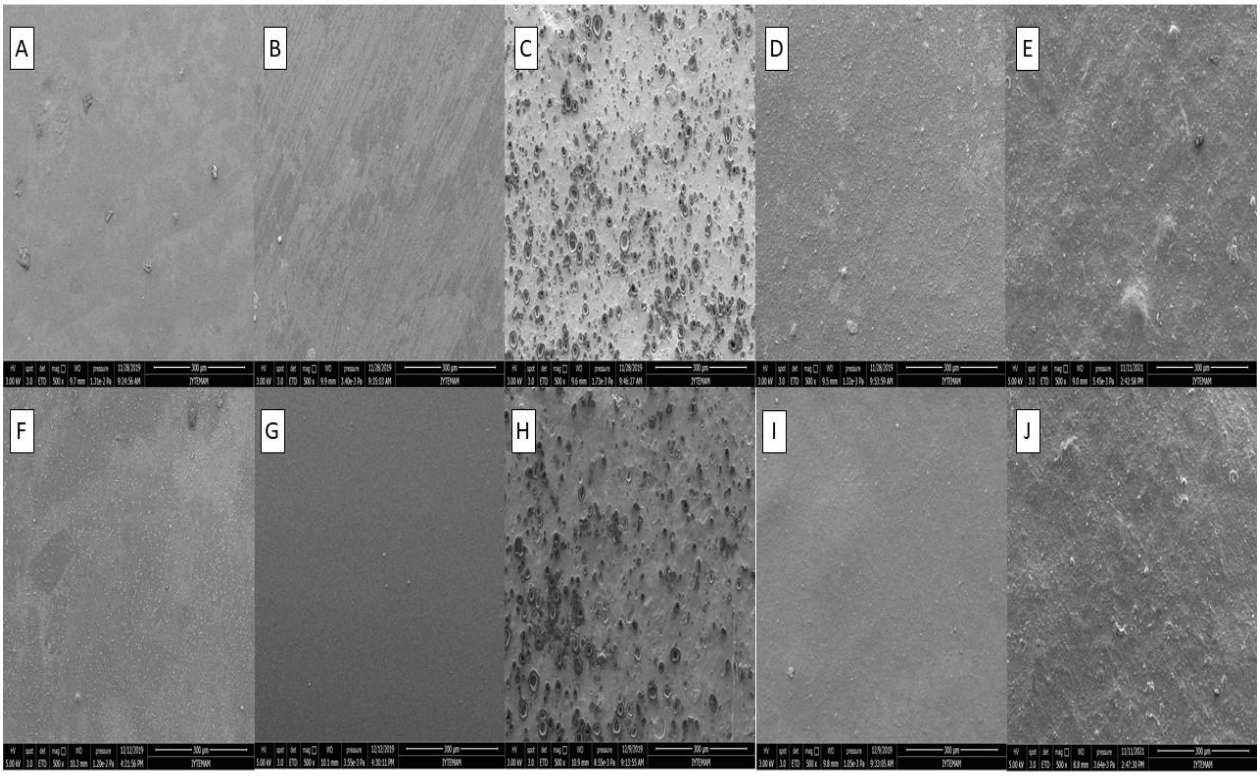

883

884 **Figure 7.** Surface morphology of pectin films: (A) CP; (B) AP; (C) FP; (D) SP; E) PSP; (F)

885 CP-Ca^{++}; (G) AP-Ca^{++}; (H) FP-Ca^{++}; (I) SP-Ca^{++}; and J) PSP-Ca^{++}. (Magnification: 500×, Scale

886 bar: 300 µm).

887

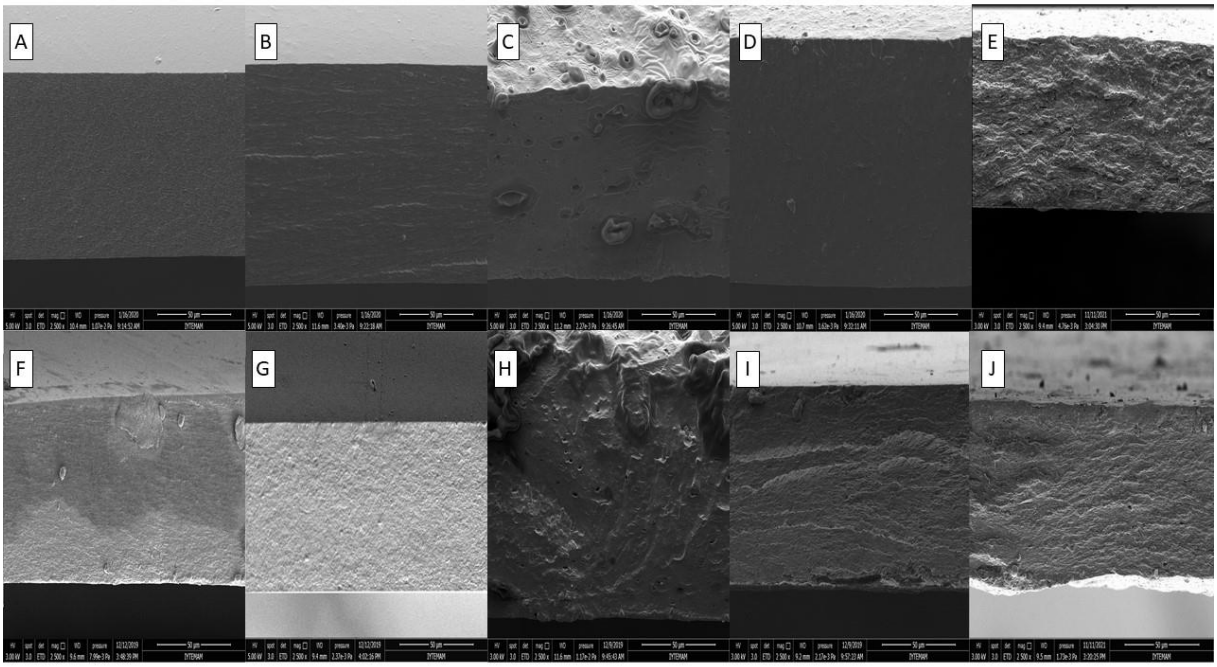

Figure 8. Cross-sectional morphology of pectin films: (A) CP; (B) AP; (C) FP; (D) SP; E) PSP; (F) CP-Ca^{++}; (G) AP-Ca^{++}; (H) FP-Ca^{++}; (I) SP-Ca^{++}; and J) PSP-Ca^{++}. (Magnification: 2500×, Scale bar: 50 µm).

900 **Table 4.** Morphological parameters of different films from AFM analysis.

Pectin film	R_{rms} (nm)[a]	R_{max} (nm)
CP	10.7 ± 1.34^{D}	84.0 ± 22.9^{DE}
AP	6.72 ± 1.81^{E}	68.2 ± 32.2^{E}
FP	11.7 ± 2.82^{CD}	82.7 ± 18.1^{DE}
SP	19.8 ± 6.16^{B}	177 ± 78.5^{AB}
PSP	22.8 ± 3.14^{AB}	157 ± 22.0^{BC}
CP-Ca^{++}	16.1 ± 1.36^{BC}	123.9 ± 23.1^{CD}
AP-Ca^{++}	7.72 ± 3.15^{E}	62.1 ± 13.8^{E}
FP-Ca^{++}	7.65 ± 2.18^{E}	59.9 ± 14.2^{E}
SP-Ca^{++}	16.4 ± 3.81^{BC}	118 ± 19.5^{CD}
PSP-Ca^{++}	31.9 ± 5.49^{A}	224 ± 27.4^{A}

901 [a] Values at each column indicated by different letters are significantly different ($p \leq 0.05$).

902

903

904

905

906

907

908

909

910 **Table 5.** Transparency and color values of pectin films.

Sample	Transparency	L*	a*	b*
CP	21.40 ± 0.17^{E}	77.27 ± 1.32^{C}	-2.68 ± 0.61^{E}	34.85 ± 2.64^{C}
AP	27.22 ± 0.02^{B}	85.84 ± 0.83^{A}	-2.96 ± 0.06^{E}	11.6 ± 1.76^{F}
FP	13.76 ± 0.30^{I}	77.77 ± 0.32^{F}	4.05 ± 0.21^{C}	42.18 ± 0.33^{A}
SP	20.01 ± 0.23^{F}	68.66 ± 0.11^{E}	2.00 ± 0.09^{D}	37.12 ± 0.37^{BC}
PSP	13.77 ± 0.85^{I}	71.78 ± 0.71^{D}	5.15 ± 0.28^{B}	30.78 ± 0.79^{D}
CP-Ca^{++}	24.83 ± 0.11^{C}	79.36 ± 1.03^{B}	1.58 ± 0.26^{D}	25.35 ± 2.11^{E}
AP-Ca^{++}	32.59 ± 0.01^{A}	85.65 ± 0.2^{A}	1.76 ± 0.07^{D}	8.02 ± 0.58^{G}
FP-Ca^{++}	17.34 ± 1.43^{G}	66.33 ± 2.79^{F}	8.48 ± 1.74^{A}	38.65 ± 2.83^{B}
SP-Ca^{++}	23.44 ± 0.09^{D}	70.49 ± 0.44^{DE}	5.73 ± 0.15^{B}	31.96 ± 0.61^{D}
PSP-Ca^{++}	15.79 ± 0.82^{H}	71.25 ± 0.66^{D}	5.42 ± 0.29^{B}	31.27 ± 0.77^{D}

911 *Data are shown as mean ± standard deviation. Data at each column indicated by different

912 letters are significantly different ($p \leq 0.05$).

913

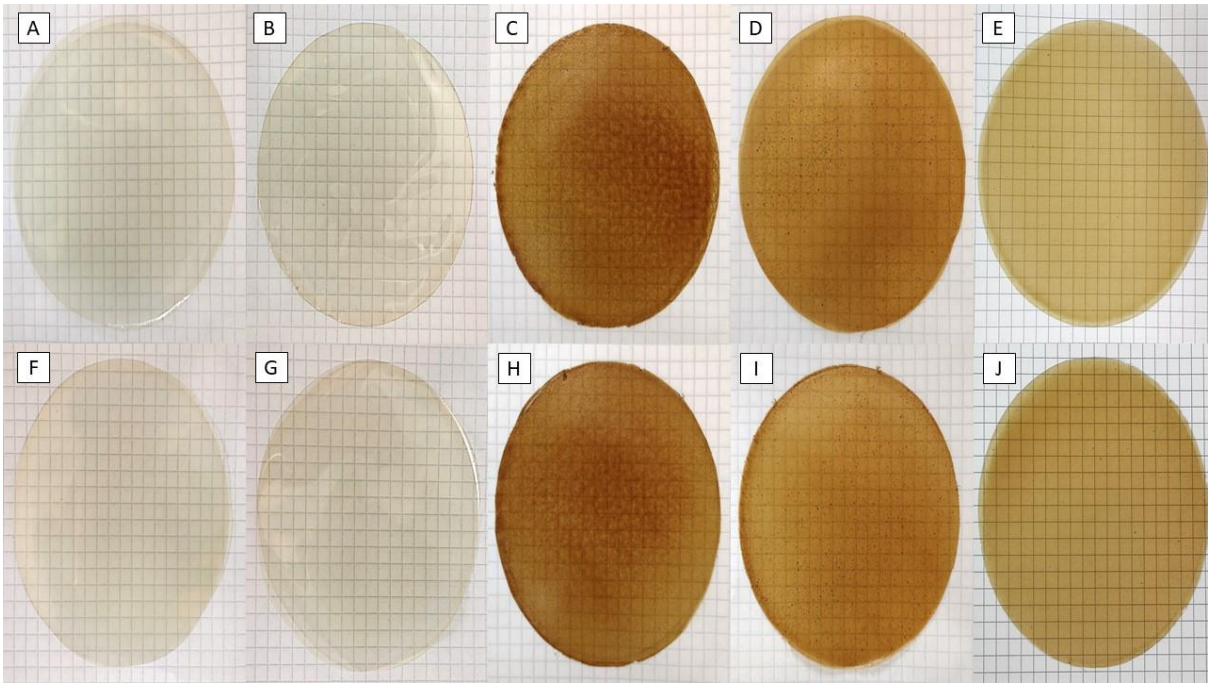

Figure 9. Digital images of pectin films. Control films: A) CP, B) AP, C) FP, D) SP, and E) PSP; cross-linked films: F) CP-Ca^{++}, G) AP-Ca^{++}, H) FP-Ca^{++}, I) SP-Ca^{++}, and J) PSP-Ca^{++}.